JOINT LTE UPLINK INTERFERENCE AND MULTIPATH SUPPRESSION FOR AERONAUTICAL TELEMETRY USING MMSE INTERFERENCE CANCELER

Shamman Noor Shoudha, Mohammad Saquib
Dept. of Electrical Engineering
The University of Texas at Dallas
800 W Campbell Rd, Richardson, TX 75080
sxn170028@utdallas.edu, Saquib@utdallas.edu

ABSTRACT

This paper addresses the use of a minimum-mean-square-error (MMSE) interference canceler for mitigating the Long-Term Evolution (LTE) uplink interference and multipath in Aeronautical Telemetry system. SOQPSK-TG modulation scheme for the telemetry victim signal and 64-QAM for the LTE interference signal are considered. For a multipath channel derived from the channel sounding data, the interference canceler achieves the target bit error rate (BER) of 10^{-5} at Carrier-to-Interference (C/I) ratio -12.7, -40.7 and -36 dB for data rates $1, 5$ and 10 Mbits/s, respectively. To offer the same performance, an MMSE channel equalizer requires C/I ratio -10.9, -25.0 and -5.0 dB.

KEY WORDS

Interference Canceler, SOQPSK-TG, LTE-A, User Equipment, Resource Blocks

INTRODUCTION

For any wireless communication link, multipath propagation is inevitable. In Aeronautical Telemetry, modulated carrier bandwidth is constantly being increased to support increased data transmission. With increasing bandwidth, multipath interference becomes the dominant link impairment for telemetry systems. In addition to multipath, telemetry users will face new challenges due to the re-allocations of radio spectrum. To meet the increasing demand for mobile data and applications, the Federal Communications Commission (FCC) Advanced Wireless Services (AWS-3) auction introduces new radio systems in the $1755 - 1780$ MHz (uplink) and $2155 - 2180$ MHz (downlink) radio spectrum [1]. According to the auction guidelines, the AWS-3 LTE uplink channel is partitioned into $1770 - 1780$ MHz and its paired downlink operates between $2170 - 2180$ MHz. The LTE uplink is the communication link from LTE user equipment (UE) to evolved NodeB (eNBs or eNodeB) base stations and the downlink is from eNodeB to LTE UEs. These AWS-3 LTE uplink

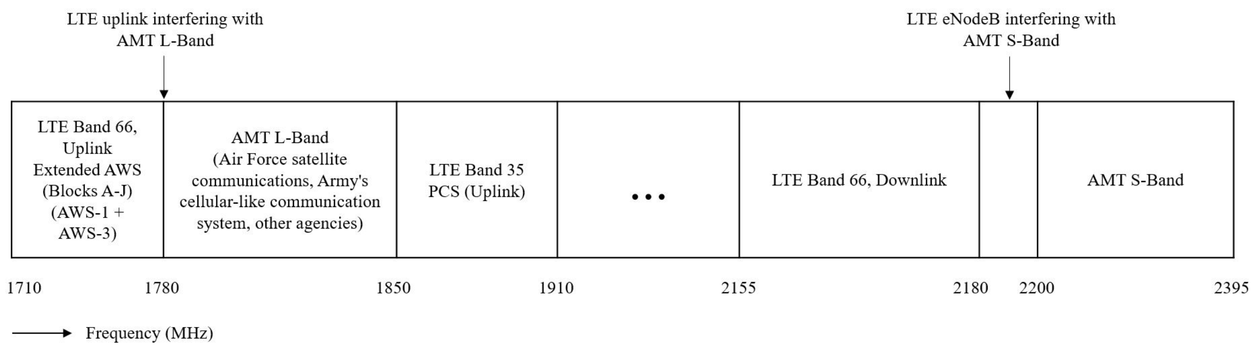

Figure 1: AWS-3 and telemetry adjacent bands.

and downlink channels are adjacent to telemetry Upper L-Band ($1780 - 1850$ MHz) and S-Band ($2200 - 2395$ MHz), respectively [2]. Adjacent LTE and telemetry spectrum are shown in Figure 1. As a result, interference from LTE uplink and downlink channels can potentially affect the operation of the physically co-located telemetry frequency bands [3]. With the growth of cellular LTE services in the above-mentioned AWS-3 bands, LTE UEs in close proximity to the telemetry ground station will severely increase the threat of LTE interference.

In [4], Kip Temple describes the impact of LTE uplink interference on telemetry systems with three IRIG-106 modulation schemes (PCM/FM, SOQPSK-TG, and ARTM CPM) at various data rates ($1, 5, 10$ and 15 Mbits/s). The hardware experiments consisted of generating of the LTE and SOQPSK signals, isolating and combining them, and then splitting the combined signal for observation, measurement, detection, and finally interference analysis. In addition to the work in [4], the effects of LTE uplink and downlink interference on telemetry S, L and C bands are demonstrated in [5]. These studies mainly considered the line-of-sight (LOS) reception of the telemetry signal.

Unlike the study of [4] and [5], our study is based on MATLAB simulation. In this work, we use MATLAB LTE Toolbox for generating LTE signals and the experimental setup in [4] as a guideline to combine the LTE and telemetry signals using MATLAB. In our analysis, to model the worst case LTE interference, line of sight (LOS) propagation is considered for LTE, whereas the desired telemetry signal suffers from multipath propagation unlike [4] and [5]. We consider the SOQPSK-TG modulation scheme for the telemetry user and apply a symbol-by-symbol detector followed by an MMSE interference canceler/channel equalizer to demodulate its signal. The performance of the channel equalizer was previously studied in [6] in absence of interference. In what follows, boldface lowercase variables denote column vectors whereas boldface uppercase variables denote matrices. For the matrix $\mathbf{M}$, $\mathbf{M}^{\mathrm{T}}$, $\mathbf{M}^{*}$ and $\mathbf{M}^{\mathrm{H}}$ denotes the transpose, conjugate and Hermitian (conjugate-transpose) of $\mathbf{M}$, respectively.

TELEMETRY SYSTEM WITH LTE INTERFERENCE

The telemetry system in the presence of LTE uplink interferer is needed to be described first to develop the MMSE interference canceler. The system considered here is summarized in Figure 2. The transmitted I/Q baseband SOQPSK-TG signal (usually called the complex-valued low-pass equivalent [7]), $s(n)$ propagates through a frequency selective multipath channel and experiences the addition of adjacent band LTE interference and additive white Gaussian noise. The resulting sequence of received samples is,

$$r_c(n) = \sum_{k=-N_1}^{N_2} h(k)s(n-k) + i(n) + \omega(n), \tag{1}$$

where, $h(n)$ is the impulse response of the unknown channel with support on $-N_1 \leq n \leq N_2$ and $i(n)$ is the complex baseband LTE signal generated using MATLAB LTE Toolbox. $\omega(n)$ is a proper [8] complex-valued white Gaussian random process with variance $\frac{\sigma_\omega^2}{2}$ per dimension [9].

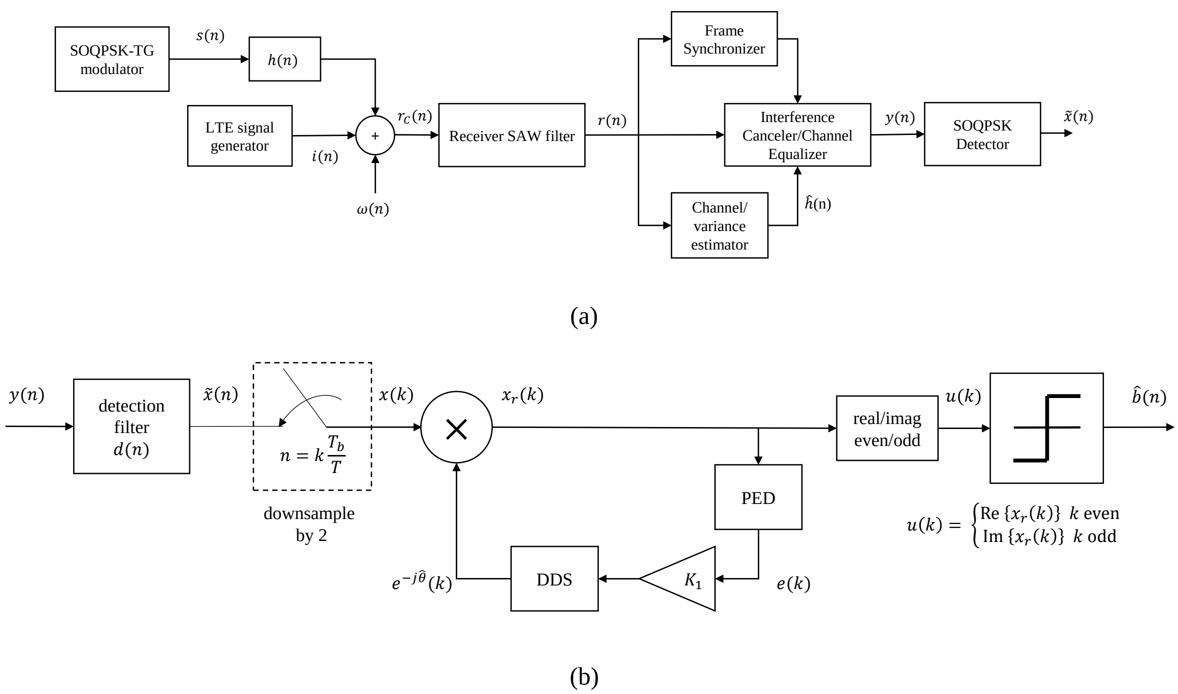

Figure 2: Block diagram: (a) Telemetry system in the presence of LTE interference, (b) SOQPSK detector.

The received signal $r_c(n)$ is filtered by the intermediate frequency (IF) surface acoustic wave (SAW) filter located in the telemetry receiver [2] to produce $r(n)$. A digital IF SAW filter is designed in the frequency domain according to the following equation centered at the AMT signal center frequency described in [4].

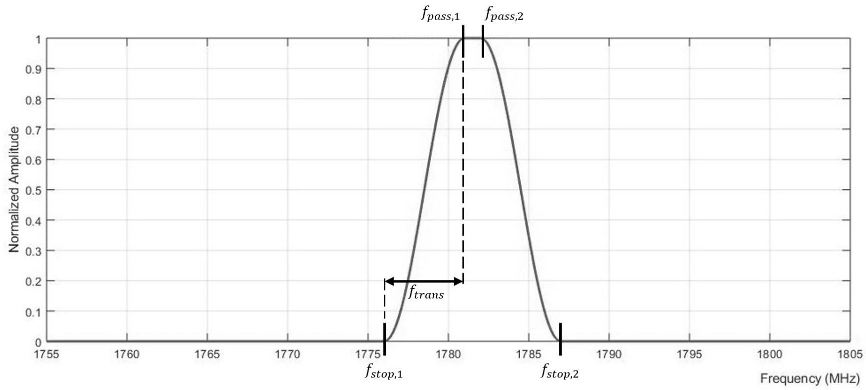

Figure 3: Digital IF SAW filter at AMT receiver with center frequency at 1781.5 MHz, $f_{\text{stop},1}$ = 1776 MHz, $f_{\text{pass},1}$ = 1781 MHz, $f_{\text{pass},2}$ = 1782 MHz, $f_{\text{stop},2}$ = 1787 MHz, f_{trans} = 5 MHz.

$$\text{H}_{\text{SAW}}(f) = \begin{cases} 0.5 - 0.5cos(\pi\eta f), & f_{stop,1} \leq f < f_{pass,1} \\ 1, & f_{pass,1} \leq f < f_{pass,2} \\ 0.5 + 0.5cos(\pi\eta f), & f_{pass,2} \leq f \leq f_{stop,2} \\ 0, & elsewhere \end{cases}, \tag{2}$$

where, $\eta = 1/f_{\text{trans}}$ and f_{trans} is the transition width of IF SAW filter (Figure 3). After filtered by the IF SAW filter, the frame synchronizer finds the starting of the iNet preamble signal. We assume perfect frame synchronization in this paper. The channel estimates of $h(n)$ for $-N_1 \leq n \leq N_2$, are then used to determine the coefficients of the MMSE filter. The MMSE filter, $c(n)$, is a linear filter that operates on the signal $r(n)$ and produces the output,

$$y(n) = \sum_{m=-L_1}^{L_2} c^*(m)r(n-m), \tag{3}$$

or in vector form,

$$\mathbf{y} = \mathbf{c}^{\text{H}}\mathbf{r}, \tag{4}$$

where, $c(n)$ is assumed to have support on $-L_1 \leq n \leq L_2$. The length of the MMSE filter will be at least 5 times larger than the channel length [10]. The following section introduces the two types of MMSE filters investigated in this paper along with the channel estimators used to compute the coefficients of these filters.

MMSE INTERFERENCE CANCELER

The MMSE filter **c** in (4) can be written in vector form [11] as,

$$\mathbf{c} = \mathbf{R}_{\text{r,r}}^{-1}\mathbf{p}, \tag{5}$$

where, $\mathbf{c}$ is the $(L_1 + L_2 + 1) \times 1$ vector of filter coefficients. Here, $\mathbf{R}_{\text{r,r}}$ is the auto-correlation matrix of the received signal and $\mathbf{p}$ is the cross-correlation of telemetry signal and the received signal. These terms can be expanded as follows,

$$\mathbf{R}_{\text{r,r}} = \text{E}[\mathbf{r}\mathbf{r}^{\text{H}}] = \mathbf{G}\mathbf{R}_{\text{s},1}\mathbf{G}^{\text{H}} + \mathbf{R}_{\text{n}}, \tag{6}$$

$$\mathbf{p} = \text{E}[\mathbf{r}\mathbf{s}^{*}] = \mathbf{R}_{\text{s},2}\mathbf{g}^{\text{H}}, \tag{7}$$

where, $\mathbf{G}$ is the $(L_1 + L_2 + 1) \times (L_1 + L_2 + N_1 + N_2 + 1)$ matrix

$$\mathbf{G} = \begin{bmatrix} h(N_2) & \dots & h(-N_1) & & & & \\ & h(N_2) & & \dots & h(-N_1) & & \\ & & & \ddots & & & \\ & & & & h(N_2) & \dots & h(-N_1) \end{bmatrix}. \tag{8}$$

$\mathbf{R}_{\text{s},1}$ and $\mathbf{R}_{\text{s},2}$ are the auto-correlation matrices of the received signal with dimensions $(L_1 + L_2 + N_1 + N_2 + 1) \times (L_1 + L_2 + N_1 + N_2 + 1)$ and $(L_1 + L_2 + 1) \times (L_1 + L_2 + 1)$, respectively. They are given as:

$$\mathbf{R}_{\text{s},1} = \begin{bmatrix} \text{R}_{\text{s}}(0) & \text{R}_{\text{s}}(-1) & \dots & \text{R}_{\text{s}}(-L_1 - L_2 - N_1 - N_2) \\ \text{R}_{\text{s}}(1) & \text{R}_{\text{s}}(0) & \dots & \text{R}_{\text{s}}(-L_1 - L_2 - N_1 - N_2 + 1) \\ \vdots & & & \vdots \\ \text{R}_{\text{s}}(L_1 + L_2 + N_1 + N_2) & \text{R}_{\text{s}}(L_1 + L_2 + N_1 + N_2 - 1) & \dots & \text{R}_{\text{s}}(0) \end{bmatrix}, \tag{9}$$

$$\mathbf{R}_{\text{s},2} = \begin{bmatrix} \text{R}_{\text{s}}(0) & \text{R}_{\text{s}}(-1) & \dots & \text{R}_{\text{s}}(-L_1 - L_2) \\ \text{R}_{\text{s}}(1) & \text{R}_{\text{s}}(0) & \dots & \text{R}_{\text{s}}(-L_1 - L_2 + 1) \\ \vdots & & & \vdots \\ \text{R}_{\text{s}}(L_1 + L_2) & \text{R}_{\text{s}}(L_1 + L_2 - 1) & \dots & \text{R}_{\text{s}}(0) \end{bmatrix}. \tag{10}$$

$\mathbf{R}_{\text{n}}$ is the $(L_1 + L_2 + 1) \times (L_1 + L_2 + 1)$ interference plus noise auto-correlation matrix given by

$$\mathbf{R}_{\text{n}} = \mathbf{R}_i + \mathbf{R}_{\omega}, \tag{11}$$

where, $\mathbf{R}_i$ is LTE interference signal auto-correlation matrix and $\mathbf{R}_{\omega} = \sigma_{\omega}^2 \mathbf{I}_{\omega}$ is the noise auto-correlation matrix. $\mathbf{g}$ is the $1 \times (L_1 + L_2 + 1)$ vector given by

$$\mathbf{g} = \begin{bmatrix} h(L_1) & \dots & h(-L_2) \end{bmatrix}. \tag{12}$$

The two types of MMSE filters investigated in this paper are MMSE Interference Canceler (MMSE-IC) and MMSE Channel Equalizer (MMSE-CE). To estimate the channel coefficients $h(n)$, Sparse

Channel Estimation (SP) and Maximum Likelihood Channel Estimation (ML) are used. Now we describe the structures of these MMSE filters.

- MMSE Interference Canceler, $\mathbf{c}_{\text{MMSE-IC}}$: From (5) and (7), the MMSE-IC filter can be written as,

$$\mathbf{c}_{\text{MMSE-IC}} = \mathbf{R}_{\text{r,r}}^{-1}\mathbf{R}_{\text{s,2}}\mathbf{g}^{\text{H}}. \tag{13}$$

  As seen from (13), the coefficients of $\mathbf{c}_{\text{MMSE-IC}}$ depend on the auto-correlation matrices $\mathbf{R}_{\text{r,r}}$ and $\mathbf{R}_{\text{s,2}}$, and channel vector $\mathbf{g}$.

- MMSE Channel Equalizer, $\mathbf{c}_{\text{MMSE-CE}}$: From (5), (6) and (7), the MMSE-CE filter can be written as,

$$\mathbf{c}_{\text{MMSE-CE}} = \left[\mathbf{G}\mathbf{R}_{\text{s,1}}\mathbf{G}^{\text{H}} + \mathbf{R}_{\text{n}}\right]^{-1}\mathbf{R}_{\text{s,2}}\mathbf{g}^{\text{H}}. \tag{14}$$

  As seen from (14), the MMSE-CE filter $\mathbf{c}_{\text{MMSE-CE}}$ depends on the auto-correlation matrices $\mathbf{R}_{\text{s,1}}$ and $\mathbf{R}_{\text{s,2}}$, and channel matrices $\mathbf{G}$ and $\mathbf{g}$. As shown in [6], MMSE-CE ignores the presence of LTE interference. So the interference plus noise auto-correlation matrix in (14) becomes,

$$\mathbf{R}_{\text{n}} = \mathbf{R}_{\omega} = \sigma_{\omega}^2\mathbf{I}_{\omega}. \tag{15}$$

  The noise variance σ_{ω}^2 is estimated in the presence of LTE interference as described in [12].

We now describe how to construct the auto-correlation matrices $\mathbf{R}_{\text{r,r}}$, $\mathbf{R}_{\text{s,1}}$ and $\mathbf{R}_{\text{s,2}}$, and the channel matrices $\mathbf{G}$ and $\mathbf{g}$.

A. *ESTIMATION OF CORRELATION MATRICES*

- Estimation of $\mathbf{R}_{\text{r,r}}$: The following equation is used to estimate $\mathbf{R}_{\text{r,r}}$ in computing the coefficients of MMSE-IC,

$$\mathbf{R}_{\text{r,r}}(k) = \frac{1}{L-k}\sum_{n=k}^{L-1} r(n)r^*(n-k); \qquad k = 0,\ldots,L-1. \tag{16}$$

- Estimation of $\mathbf{R}_{\text{s,1}}$, $\mathbf{R}_{\text{s,2}}$: A pre-computed auto-correlation signal using random SOQPSK-TG symbols is used as R_{s} in (9) and (10) to compute approximations of the auto-correlation matrices $\mathbf{R}_{\text{s,1}}$ and $\mathbf{R}_{\text{s,2}}$ [6]. For SOQPSK-TG, the correlation function has the most significant values for delay $-5 \leq k \leq 5$ [13].

B. *ESTIMATION OF CHANNEL COEFFICIENTS*

- ML Channel Estimation: If the telemetry channel $h(n)$ is assumed to have supports on $-N_1 \leq n \leq N_2$, the ML estimate [14] of the channel is,

$$\hat{\mathbf{h}}_{\text{ML}} = (\mathbf{P}^{\text{H}}\mathbf{P})^{-1}\mathbf{P}^{\text{H}}\mathbf{r}, \tag{17}$$

  where, $\mathbf{P}$ is a matrix of size $(L_p - N_1 - N_2) \times (N_1 + N_2 + 1)$ consisting of the pilot sequence of telemetry standard, where L_{P} denotes the number of SOQPSK samples corresponding to the preamble plus ASM bits.

- Sparse Channel Estimation: Sparse estimation of the telemetry channel is based on a sensing matrix [13]. The sensing matrix comprises samples of SOQPSK-TG based on the telemetry pilot bit sequence currently defined in the aeronautical telemetry standard.

  If it is known a priori that the **h** is S-sparse, i.e., $\| \mathbf{h} \|_0 = S$, then ML solution for **h** in (17) is of the form,

$$\hat{\mathbf{h}}_{\text{SP}} = \min_{\text{h} \in \text{C}^{N_1+N_2+1}} \| \mathbf{y} - \mathbf{X}\mathbf{h} \|_2^2 \text{ such that } \| \mathbf{h} \|_0 = S. \quad (18)$$

  The solution requires a search over all $\binom{N_1+N_2+1}{S}$ possibilities for the S positions of non-zero elements in **h**.

For our application, we use $L_{\text{p}} = 2 \times (128 + 64) = 384$ and $2 \times 6144 = 12288$ SOQPSK samples corresponding to the 6144 data bits. The telemetry channel has $N_1 = 12$ non-causal samples and $N_2 = 25$ causal samples. The filter **c** has $L_1 = 3 \times N_1 = 36$ non-causal samples and $L_2 = 3 \times N_2 = 75$ causal samples. The numerical results using the proposed methods of channel estimation and interference cancellation are illustrated in the next section.

NUMERICAL RESULTS

The Sparse and the ML channel estimators described in the previous section yield quite similar BER performances for either of the MMSE filters. However, the sparse estimator performs slightly better than the ML estimator for MMSE-IC and vice versa for MMSE-CE. So the BER performances of MMSE-IC with Sparse channel estimation and MMSE-CE with ML channel estimation are assessed using our MATLAB simulation environment. For the telemetry victim signal, the IRIG-106 modulation scheme SOQPSK-TG is tested at data rates $1, 5$ and 10Mbits/s operating in single-path and multipath environments. For the LTE interfering signal, the number of user equipment (UE) is 1, the resource block allocation for the UE is 10, the modulation scheme was 64-QAM. The parameters of SOQPSK and LTE signals are given in Table 1. The multipath environment is based on the flight-line channels captured at Edwards AFB, CA, which is shown in Figure 4.

The LTE uplink interferer has a 10 MHz bandwidth with a fixed center and boundary frequencies. The telemetry victim signal is also fixed in frequency. The band-edge back off from 1780 MHz is dependent on the data rate and modulation mode of the telemetry signal [2]. Therefore, to introduce LTE interference into the victim telemetry signal, the Carrier (the telemetry signal) to Interference (the LTE signal) ratio (C/I) is varied. The power of the additive white Gaussian noise is scaled to achieve a signal-to-noise ratio (SNR) of 20 dB. The simulated BER performance versus the C/I ratio for different data rates are shown in Figure 5. We observe that for the selected multipath channel, the target BER is achieved by MMSE-IC at C/I ratio $12.7, 40.7$ and 36 dB for data rates $1, 5$ and 10 Mbits/s, respectively. MMSE-CE achieves the same BER at C/I ratio $10.9, 25.0$ and 5.0 dB. These observations are tabulated in Table 2.

Telemetry Signal		**LTE Signal**	
Data rate (Mbits/s)	$1, 5, 10$	Sampling rate (MHz)	15.36
Modulation	SOQPSK-TG	Modulation	64-QAM
Center frequency (MHz)	$1781.5, 1785, 1790$	Center frequency (MHz)	1775
Frame structure	iNet	Data length (bits)	100
Data length (bits)	6144	Total resource blocks	50
ASM length (bits)	64	Channel bandwidth (MHz)	10
Preamble length (bits)	128	LTE Protocol	A3-5
		Number of UE	1
		Occupied RBs	10
		Occupied bandwidth (MHz)	10

Table 1: Simulation parameters for SOQPSK-TG and LTE signals.

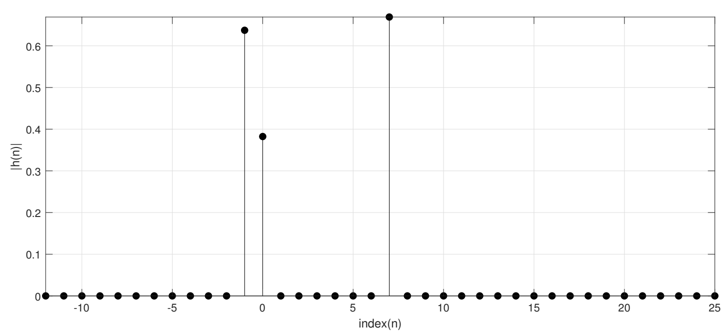

Figure 4: Telemetry multipath channel.

CONCLUSIONS

This paper investigated the effectiveness of MMSE interference canceler that jointly suppresses adjacent band LTE uplink and multipath interferences for aeronautical telemetry users. This study is based on MATLAB simulation. We considered SOQPSK-TG modulated scheme for the telemetry victim signal and 64-QAM for the LTE interference signal. For a multipath channel captured at Edwards AFB CA, it is observed that depending on the SNR and target BER, the MMSE canceler provides C/I gains of $1.8, 15.7$ and 31.0 dB over the MMSE channel equalizer for $1, 5$ and 10 Mbits/s, respectively. These gains were primarily attributed to the frequency selectivity of the channel. This work assumed perfect frame synchronization. However, frame synchronization is always an issue in the presence of interference. A joint study of frame synchronization and interference cancellation is necessary and left as our future work.

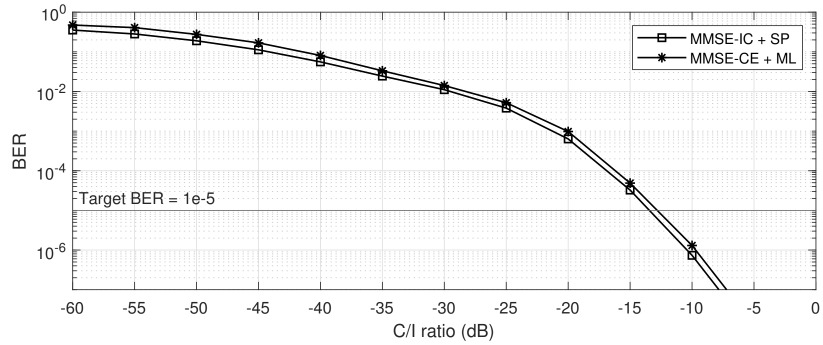

(a) Telemetry data rate = 1 Mbits/s.

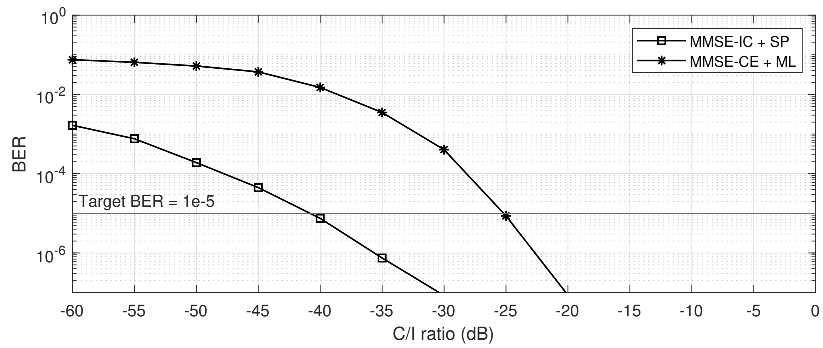

(b) Telemetry data rate = 5 Mbits/s.

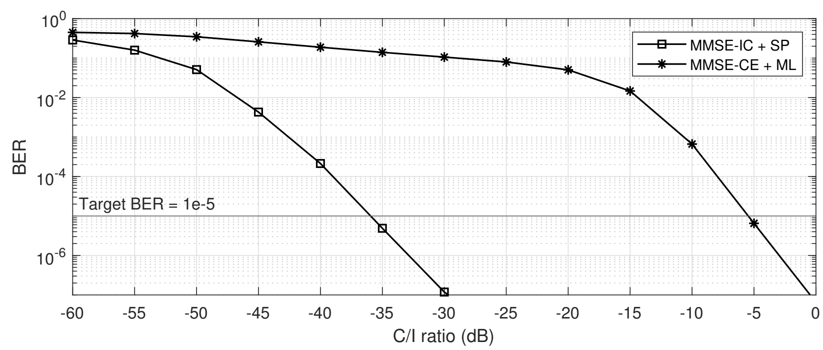

(c) Telemetry data rate = 10 Mbits/s.

Figure 5: Simulated BER vs C/I ratio (dB) performance of MMSE-IC and MMSE-CE for telemetry multipath channel in Figure 4 and SNR = 20 dB.

Telemetry data rate (Mbits/s)	C/I ratio at target BER using IC (dB)	C/I ratio at target BER using CE (dB)
1	-12.7	-10.9
5	-40.7	-25.0
10	-36.0	-5.0

Table 2: C/I ratio (dB) at target BER of 10^{-5}.

REFERENCES

[1] F. C. Commission *et al.*, "In the Matter of Amendment of the Commissions Rules With Regard to Commercial Operations in the 1695-1710 MHz, 1755-1780 MHz and 2155-2180 MHz Bands," *Report and Order*, pp. 13–185, 2014.

[2] R. C. C. Secretariat, "Transmitter and Receiver Systems."

[3] L. ETSI, "Evolved universal terrestrial radio access (e-utra); user equipment (ue) radio transmission and reception," *ETSI TS*, vol. 136, no. 101, p. 16, 2017.

[4] K. Temple, "An Initial Look at Adjacent Band Interference Between Aeronautical Mobile Telemetry and Long-Term Evolution Wireless Service," tech. rep., AIR FORCE TEST CENTER Edwards AFB United States, 2016.

[5] J. F. Gonzalez, M. Elahi, J. A. Castillo, V. Gonzalez, P. Corral, and S. Yasuda, "4G LTE AND TELEMETRY INTERFERENCE ANALYSIS ON A FLEXIBLE SOFTWARE-DEFINED RADIO TESTBED PLATFORM," 2018.

[6] M. Rice, M. S. Afran, and M. Saquib, "MMSE Equalization of Aeronautical Telemetry Channels," tech. rep., BRIGHAM YOUNG UNIV PROVO UT DEPT OF ELECTRICAL AND COMPUTER ENGINEERING, 2014.

[7] U. Madhow, *Fundamentals of digital communication*. Cambridge University Press, 2008.

[8] P. J. Schreier and L. L. Scharf, *Statistical signal processing of complex-valued data: the theory of improper and noncircular signals*. Cambridge university press, 2010.

[9] F. D. Neeser and J. L. Massey, "Proper complex random processes with applications to information theory," *IEEE transactions on information theory*, vol. 39, no. 4, pp. 1293–1302, 1993.

[10] M. Rice, M. S. Afran, and M. Saquib, "Equalization in Aeronautical Telemetry using Multiple Transmit Antennas," *IEEE Transactions on Aerospace and Electronic Systems*, vol. 51, pp. 2148–2165, July 2015.

[11] M. H. Gruber, "Statistical Digital Signal Processing and Modeling," 1997.

[12] M. Rice, M. Saquib, and E. Perrins, "Estimators for inet-formatted soqpsk-tg," tech. rep., AIR FORCE TEST CENTER EDWARDS AFB CA, 2014.

[13] M. Rice, C. Hogstrom, M. S. Afran, and M. Saquib, "On Sparse Channel Estimation in Aeronautical Telemetry," *IEEE Transactions on Aerospace and Electronic Systems*, 2019.

[14] M. Rice, M. Saquib, A. Cole-Rhodes, F. Moazzami, and E. Perrins, "Phase 1 final report: Preamble Assisted Equalization for Aeronautical Telemetry (PAQ)," 2014.